

Frequency-Domain Decomposition and Deep Learning Based Solar PV Power Ultra-Short-Term Forecasting Model

Jichuan Yan, Lin Hu, Zhao Zhen, *Member, IEEE*, Fei Wang, *Senior Member, IEEE*, Gang Qiu, Yu Li, Liangzhong Yao, Miadreza Shafie-khah, *Senior Member, IEEE*, João P. S. Catalão, *Senior Member, IEEE*

Abstract—Ultra-short-term photovoltaic (PV) power forecasting can support the real-time dispatching of power grid. However, PV power has great fluctuations due to various meteorological factors, which increases energy prices and cause difficulties in managing the grid. This paper proposes an ultra-short-term PV power forecasting model based on optimal frequency-domain decomposition(FDD) and deep learning. First, the optimal frequency demarcation points for decomposition components are obtained through frequency domain analysis. Then the PV power is decomposed into the low-frequency and high-frequency components, which supports the rationality of decomposition results and solves the problem that the current decomposition model only uses the direct decomposition method and the decomposition components are not physical. Then convolutional neural network(CNN) is used to forecast the low-frequency and high-frequency components, and final forecasting result is obtained by addition reconstruction. Based on actual PV data in heavy rain days, the MAPE of the proposed forecasting model is decreased by 52.97%, 64.07% and 31.21%, compared with discrete wavelet transform, variational mode decomposition and direct prediction models. In addition, compared with Recurrent neural network and Long-short-term memory model, the MAPE of CNN forecasting model is decreased by 23.64% and 46.22%, and the training efficiency of CNN forecasting model is improved by 85.63% and 87.68%. The results fully show that the proposed model in this paper can improve both the forecasting accuracy and time efficiency significantly.

This work was supported by the National Key R&D Program of China (Technology and application of wind power/photovoltaic power prediction for promoting renewable energy consumption, 2018YFB0904200) and eponymous Complement S&T Program of State Grid Corporation of China (SGLNDK00KJJS1800266). (*Corresponding author: Fei Wang.*)

J. Yan, L. Hu and F. Wang are with the Department of Electrical Engineering, North China Electric Power University, Baoding 071003, China; F. Wang is also with the State Key Laboratory of Alternate Electrical Power System with Renewable Energy Sources (North China Electric Power University), Beijing 102206, China, and also with the Hebei Key Laboratory of Distributed Energy Storage and Microgrid (North China Electric Power University), Baoding 071003, China (e-mail: yjc@ncepu.edu.cn; linhu@ncepu.edu.cn; feiwang@ncepu.edu.cn).

Z. Zhen is with the State Key Lab of Power System, Department of Electrical Engineering, Tsinghua University, Beijing 100084, China; also with the Department of Electrical Engineering, North China Electric Power University, Baoding 071003, China (e-mail: zhenzhao@mail.tsinghua.edu.cn).

G. Qiu and Y. Li are with the Dispatch and Control Center, State Grid Xinjiang Electric Power Co., Ltd, Urumqi 830018, China (e-mail: qiugang412@163.com; liyu@xj.sgcc.com.cn).

L. Yao is with the School of Electrical Engineering and Automation, Wuhan University, Wuhan 430072, China (e-mail: yaoliangzhong@hotmail.com).

Miadreza Shafie-khah is with School of Technology and Innovations, University of Vaasa, Vaasa 65200, Finland, (e-mail: mshafiek@univaasa.fi).

João P. S. Catalão is with the Faculty of Engineering of the University of Porto and INESC TEC, Porto4200-465, Portugal (e-mail: catalao@fe.up.pt).

Keywords—PV power forecasting, ultra-short term, frequency domain, decomposition, deep learning

I. INTRODUCTION

1.1 Background and motivation

Facing the shortage of fossil energy and the deterioration of climate such as greenhouse effect, ozone hole and melting of polar glaciers, sustainable development of energy and environment has attracted worldwide attention. Due to the advantages of sustainability, clean and pollution-free, high flexibility, etc., PV power generation technology and related industries have experienced tremendous growth in the past few years [1-3]. PV power affected by various meteorological factors is highly uncertain. These fluctuations will cause energy prices, grid management difficulties, etc. which will affect stable operation of the power grid[4-5]. PV power generation system is typically connected to the power grid to compensate for losses in conventional power generation systems. In a grid, some power generation systems that output constant power are called conventional power plants. Others convert their power in response to changes of PV generation and demand, which balances total power consumption with total power generation. These power plants that convert output power are called load-tracking power plants. When the output power of PV generation system is markedly increased or decreased, the load-tracking power plants must respond promptly. PV power forecast for the 15 min in advance enables the load-tracking power plant to react to sudden output changes timely. In order to stabilize the operation of the power grid, ultra-short-term PV power prediction is particularly significant [6-8].

1.2 literature review

Due to various meteorological factors, the photovoltaic power has great fluctuations [9-11]. It is difficult to achieve satisfactory results with traditional prediction methods. In recent years, the method of first decomposing and then predicting photovoltaic power data has become a research hotspot. Among them, frequency-domain decomposition method excavates and extract PV power characteristics from the perspective of the frequency domain, which has become a current research hotspot. Literature [12] uses the variational mode decomposition (VMD) to decompose different frequency components from the historical PV power time series. Literature [13] decomposed the time series of solar photovoltaic power generation by wavelet decomposition. Literature [14] proposed a new prediction model based on Hilbert Huang Transform (HHT) and integrating improved empirical mode decomposition (IEMD) with feature selection and prediction engine. IEMD is used to decompose data. In the above literature, the data are only decomposed using existing models, but few literatures can support the rationality of the decomposition results through an effective method.

Table I lists various methods of solar photovoltaic power generation forecasting, which can be summarized into the following categories: physical methods, statistical methods, and intelligent algorithms[15]. Among the physical methods[16], the three basic methods are Numerical weather forecast model, total sky image and satellite image model based on cloud movement, which can help estimate photovoltaic power. However, physical methods require detailed historical data to train prediction models, relying on detailed power plant geographic information and accurate meteorological data. The physical formula has certain errors, and its model has poor anti-interference ability and weak robustness. Common statistical methods[17] include time series method, regression analysis method, grey theory, fuzzy theory and spatiotemporal correlation method. Compared to physical methods, statistical methods are simpler, which do not need to consider photovoltaic system parameters and complex photoelectric conversion models. However, statistical methods often need to collect and process a large amount of historical data, which increases the difficulty of data acquisition and processing. Common intelligent methods[18-20] include artificial neural network, support vector machine, Markov chain and particle swarm algorithm. The intelligent method does not need to obtain a specific expression between input and output, and obtains a prediction model of photovoltaic power generation output through training on historical data, which is simple to operate and easy to implement, but has the defects of over-learning and easy to fall into local optimal solutions. Compared with the above-mentioned traditional intelligent algorithms, deep learning (DL)[21-23] algorithms are more promising. There are various branches in the deep learning system, including recurrent neural network (RNN), long and short-term memory network (LSTM) and convolutional neural network (CNN). Among them, CNN is not only successfully applied to image processing, but also used to solve one-dimensional data classification and regression problems. CNN reduces the parameters to be estimated due to the weight sharing technology, thereby shortening the training time for prediction.

And CNN can perform feature extraction on the data, which has good robustness. And there are few studies on the application of CNN to the ultra-short-term prediction of photovoltaic power, so this paper is dedicated to the reasonable application of the CNN algorithm to improve the accuracy of the ultra-short-term prediction of photovoltaic power.

1.3 Contribution

To overcome the shortcomings that there is currently no effective method to support the rationality of the frequency domain decomposition results, this paper proposes an ultra-short-term prediction model of PV power based on optimal frequency-domain decomposition and deep learning. First, the amplitude and phase of each frequency sine wave is obtained by fast Fourier decomposition. As the frequency demarcation point is different, the correlation between the decomposition component and the original data is analyzed. By analyzing the prediction results of the decomposition components at different frequency demarcation points, the optimal frequency demarcation points for decomposing low-frequency components and high-frequency components are obtained. Then convolutional neural network is used to predict low-frequency component and high-frequency component, and final prediction result is obtained by addition reconstruction.

The main contributions of this paper include:

(1) By minimizing the square of the difference that the correlation between low-frequency components and raw data is subtracted from the correlation between high-frequency components and raw data, the optimal frequency demarcation points for decomposition components are obtained, and the PV power is decomposed into the low frequency components and high-frequency components. The low-frequency component represents the regular part of PV power generation, which shows PV power's trend characteristics, while the high-frequency component represents the randomness of photovoltaic power generation, which shows PV power's fluctuation characteristics affected by other factors such as weather. This method supports the rationality of the

TABLE. I. DEVELOPMENT OF PHOTOVOLTAIC POWER PREDICTION TECHNOLOGY

| Author | Years | Predictive model | Description |
|--------------------|-------|--------------------|--|
| Wang, et al.[16] | 2018 | Physical model | A cloud motion displacement vector calculation method based on the invariance of image phase shift by the Fourier phase correlation theory is proposed to predict solar power generation on a small time scale. |
| Zhong, et al. [17] | 2017 | Grey theory | A multivariate grey theory model based on particle swarm optimization algorithm is proposed to forecast short-term photovoltaic power generation. |
| Liu, et al. [18] | 2015 | BP neural Networks | Use BP with ANN model to predict the future photovoltaic power generation. The prediction accuracy exceeds the conventional artificial neural networks. |
| Lu and Chang[19] | 2018 | RBFNN | A hybrid RBFNN model with data regularity scheme was developed for photovoltaic output prediction. |
| Sun, et al. [20] | 2015 | SVM | A short-term stepwise temperature prediction model for photovoltaic modules based on support vector machines is proposed. Under the same conditions, the stepwise prediction model has better accuracy than the direct prediction model. |
| Qing and Niu[21] | 2018 | LSTM | The LSTM model was developed to predict solar irradiance in advance based on weather data. |
| Wang, et al[22] | 2020 | LSTM-RNN | An independent day-ahead photovoltaic power generation prediction model based on long-term short-term memory recurrent neural network was established. |
| Huang, et al[23] | 2020 | CNN | A method for forecasting day-ahead probability PV power based on improved quantile CNN is proposed. |

decomposition results and solves the problem that the current decomposition model only uses the direct decomposition method, and the decomposition components are not physical.

(2) CNN is not only successfully applied to image processing, but also used to solve one-dimensional data classification and regression problems. CNN reduces the parameters to be estimated due to the weight sharing technology, thereby shortening the training time for prediction. CNN can perform feature extraction with good robustness. Therefore, this article is dedicated to the reasonable application of CNN to improve the accuracy and efficiency of ultra-short-term prediction of PV power.

(3) The method proposed in this paper is verified by the data of PV power station in Ningxia and Jilin in China on sunny days, cloudy days, light rainy days and heavy rainy days. The results show that the proposed model improves the prediction accuracy.

The rest of this article is organized as follows. Section 2 introduces the theory of FFT and deep learning. Section 3 introduces how to choose the optimal frequency demarcation point of frequency-domain decomposition. In section 4, the details of the experimental simulation are introduced and the relevant analysis results are discussed. The conclusions are drawn in Section 5.

II. METHODOLOGY

2.1 Fast Fourier Transform

Discrete Fourier Transform (DFT) can discretize the frequency domain of a finite-length sequence, but its computational complexity is too large to process the problem in real time, thus leading to the Fast Fourier Transform (FFT) [24-26]. FFT uses the periodicity and symmetry to improve the DFT algorithm, which greatly reduces the amount of computation. The sine wave decomposed by FFT is the most single frequency signal. Any complex signal can be seen as the composite of many sine waves with various frequencies and amplitudes. It can be considered that sine wave is the basis of all waveforms. Therefore, this paper uses FFT to decompose PV power in the frequency domain. Fig. 1 shows the relationship between the time domain signal and the sine wave signals of different frequencies. The black curve represents the time domain signal of a PV power curve, and the color curves represent the sine wave signals of different frequencies that make up this PV power curve.

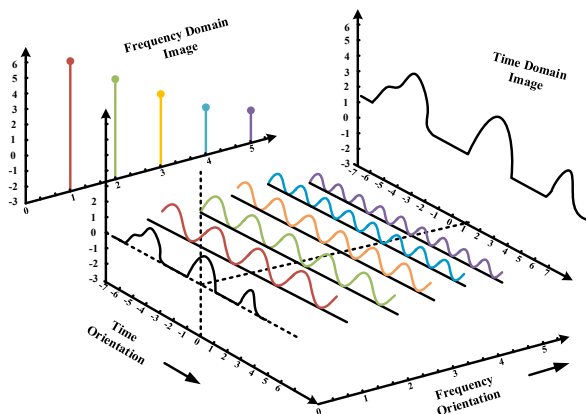


Fig. 1. Relationship between time domain signals and sine wave signals of different frequencies

According to Eq. (1), discretized sequence is decomposed into signals of multiple frequencies. and the sine wave and the cosine wave of the same frequency are superimposed by different coefficients to generate cosine waves of various phases of the same frequency. The modulus c_n of complex number in the frequency domain obtained by FFT represents the energy of the cosine wave corresponding frequency, and the angle of the complex number represents the phase θ_n of the cosine wave, thereby obtaining the amplitude spectrum and the phase spectrum. The actual amplitude a_k of the k -th point of the cosine is defined by Eq. (2). The physical frequency f_k of the k -th point is calculated as Eq. (1).

$$f(n) = a_0 + \sum_{n=1}^N [a_n \cos(2\pi f_n) + b_n \cos(2\pi f_n)] \quad (1)$$

$$= c_0 + \sum_{n=1}^N c_n \cos(2\pi f_n + \theta_n)$$

$$a_k = \frac{2c_k}{N} \quad (2)$$

$$f_k = k * \frac{f_s}{N} \quad (3)$$

In the formula, n is a positive integer. a_0 is constant component, a_n is the cosine component amplitude and b_n is the sinusoidal component amplitude. Where c_0 is the constant component, c_n is the amplitude, $f_n = \frac{2\pi n \Delta t}{N}$ is the frequency, θ_n is the phase, N is a positive integer, and Δt is the sampling interval.

2.2 Pearson correlation coefficient

Pearson's correlation coefficient (R) represents the curve fit of two sequences. Specifically, the critical criterion for R is a very strong correlation between 0.8 and 1.0, a strong correlation between 0.6 and 0.8, a medium correlation between 0.4 and 0.6, a weak correlation between 0.2 and 0.4, and very weak correlation or no correlation between 0 and 0.2[27]. R is defined as shown in Eq. (4):

$$R_{X,Y} = \frac{N \sum XY - \sum X \sum Y}{\sqrt{N \sum X^2 - (\sum X)^2} \sqrt{N \sum Y^2 - (\sum Y)^2}} \quad (4)$$

2.3 Convolutional neural network

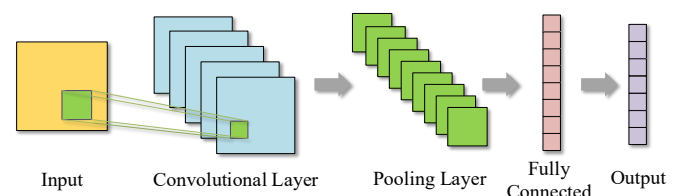


Fig. 2. The structure of convolutional neural network

Convolutional Neural Network (CNN) is a common deep learning model with powerful feature extraction capabilities. CNN generally consists of five types of cell layers, namely the input layer, the convolutional layer, the pooling layer, the fully

connected layer, and the output layer [28]. The structure of CNN is shown in Fig. 2.

2.3.1 Convolution layer

The role of the convolutional layer is to extract features from the input information. The convolutional layer is typically composed of multiple convolution kernels, each of which is used to compute a feature map. Each cell of the feature map is connected to the region of the adjacent cell in the previous layer. Convolution of the input by the convolution kernel and nonlinear processing of convolution results by activation function can acquire the new feature map. The formula for the convolutional layer is shown by Eq. (5)

$$y_{i,j,k}^l = F((w_k^l)^T x_{i,j}^l + b_k^l) \quad (5)$$

Where w_k^l and b_k^l are the weights and bias of the k -th convolution kernel in the l -th convolutional layer, respectively. $x_{i,j}^l$ is the input information of (i,j) region in the l -th convolution layer. The weight w_k^l in the l -th convolution layer is shared by each region of the input information, which is weights sharing. $F(\bullet)$ is the activation function applied to the convolution layer, which can effectively improve the fitting ability of the model.

2.3.2 Pooling layer

The role of the pooling layer is to reduce the size of the feature map generated by the convolution layer, and to effectively extract the feature information in the feature map. The formula for pooling layer is shown by Eq. (6)

$$P_{i,j,k}^l = pool(y_{m,n,k}^l) \quad (6)$$

Where $(m,n) \in R_{i,j}$, and $R_{i,j}$ are the information at location (i,j) .

2.3.3 Fully connected layer

The function of the fully connected layer is to summarize the distributed feature representations learned by the previous layer into the same space for subsequent applications. All the neurons in the previous layer are connected to each neuron in the current layer.

2.3.4 Description of one-dimensional CNN

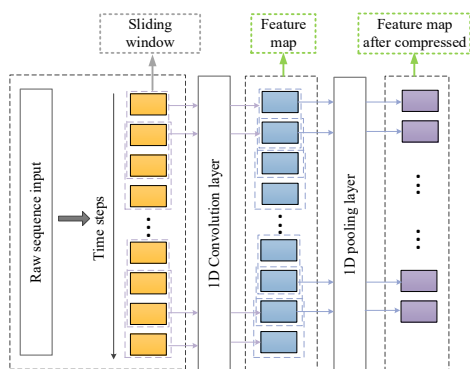


Fig. 3. Illustration of 1D convolution and 1D pooling

One-dimensional(1D) CNN is a branch of CNN[29]. The convolution kernel window of CNN1D slides in a single direction (i.e. time step). Because photovoltaic power is time series data, this paper chooses CNN1D to build prediction model. In the 1D convolution layer, the size of kernel is 3 and the corresponding stride is 1. In the 1D pooling layer, the size of kernel is 2 and the corresponding stride is 1. The specific flow chart is shown in Fig. 3.

2.4 Combined Model Framework

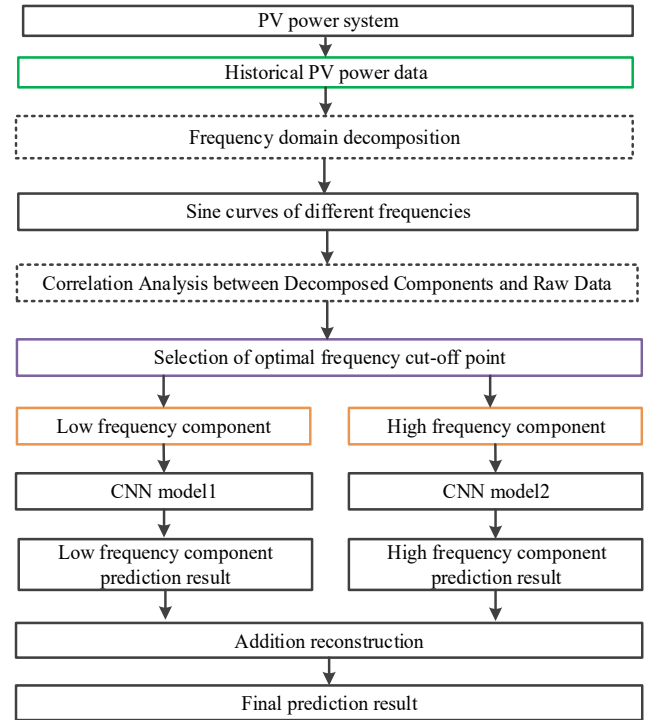


Fig. 4. Ultra-short-term prediction model of PV power based on optimal frequency-domain decomposition and deep learning

The framework of ultra-short-term prediction model of PV power based on optimal frequency-domain decomposition and deep learning proposed in this paper is shown in Fig. 4. First, the amplitude and phase of each frequency sine wave is obtained by fast Fourier decomposition. As the frequency demarcation point is different, the correlation between the decomposition component and the original data is analyzed. By minimizing the square of the difference that the correlation between low-frequency components and raw data is subtracted from the correlation between high-frequency components and raw data, the optimal frequency demarcation points for decomposition components are obtained. Then convolutional neural network is used to predict low-frequency component and high-frequency component, and final prediction result is obtained by addition reconstruction.

III. SPECTRUM ANALYSIS

3.1 Frequency domain decomposition

This paper selects the PV data of Ningxia PV Power Station in China from 0:00 on January 1 in 2017 to 23:45 on November 30 in 2017 to train the model, and perform frequency domain decomposition through FFT to obtain the amplitude spectrum and phase spectrum of PV power, which are shown in Fig. 5 and Fig. 6.

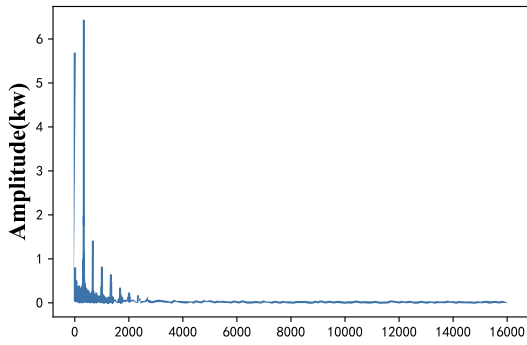


Fig. 5. Amplitude spectrum of PV power

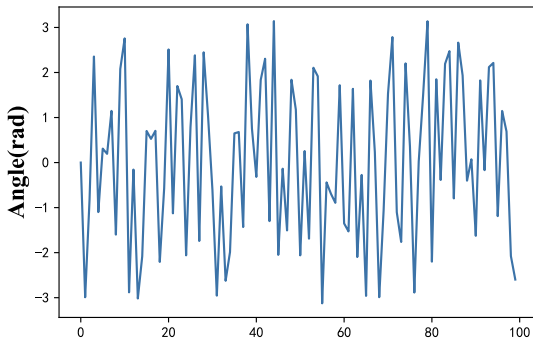


Fig. 6. Phase spectrum of PV power

3.2 Selection of optimal frequency demarcation point

Through FFT spectrum analysis, PV power can be decomposed into low-frequency components and high-frequency components. The low-frequency component represents the regular part of PV power, which indicates its trend characteristics, while the high frequency component represents the randomness of PV power, which indicates its fluctuation characteristics affected by other factors such as weather. How to accurately decompose low-frequency components and high-frequency frequencies has always been a difficult problem. In order to solve this problem, this article chooses the optimal frequency demarcation point from the perspective of the correlation between decomposed data and raw data. Fig. 7 shows the correlation between decomposed components and raw data. When frequency-domain decomposition is performed on PV power data, the more frequencies selected, the stronger the correlation between low-frequency components and raw data, and the weaker the correlation between high-frequency components and raw data.

To illustrate the effect of the correlation between the decomposition component and raw data on the prediction results, this paper uses the CNN model to predict low-frequency components and high-frequency components from 0:00 on January 1 in 2017 to 23:45 on November 30 in 2017. Table II compares prediction results of low-frequency and high-frequency components at different frequencies. The frequency demarcation point selected in Table II is the frequency node with relatively large amplitudes in amplitude spectrum of Fig. 5. As the correlation between the low-frequency component and raw data increases, the curve fitting

effect becomes better. As the correlation between the high-frequency component and raw data decreases, the curve fitting effect becomes worse. The relationship between the selected frequencies and the correlation of decomposition component and raw data shows that as the frequency number increases, the better prediction result of the low-frequency component and the worse prediction result of the high-frequency component, so the two are contradictory. Low-frequency components represent the regular part of PV power which can be accurately predicted, while high-frequency components are relatively random, which are difficult to predict. If the proportion of low-frequency components in raw data can be increased, accurate prediction of low-frequency components to balance prediction errors of high-frequency components will effectively improve the overall prediction accuracy. Therefore, the idea of optimal frequency demarcation point selection proposed in this article is that low-frequency component consider to select the highest frequency demarcation point as possible, and accounts for a large proportion, and then the second-level is that high-frequency component, which hope the frequency selection is not too high. Otherwise, prediction is too difficult to get a certain level of balance.

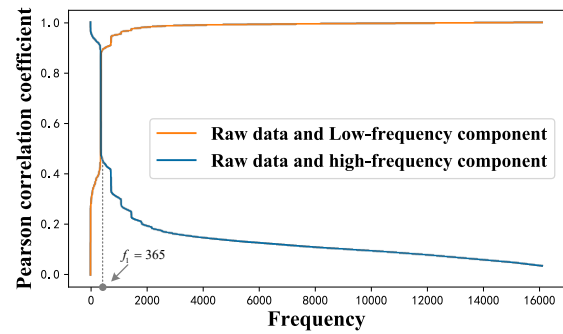


Fig. 7. Correlation between decomposition components and raw data before weighting

From Fig. 7, it can be seen that when the frequency reaches a certain value, as the frequency band increases, the correlation between low-frequency components and raw data does not increase significantly. It can be considered that there is no significant increase in the correlation between low-frequency components and raw data, while the correlation between high-frequency component and raw data continues to decline. This optimal frequency demarcation point that balances both low-frequency components and high-frequency components not only ensures sufficient extraction of low-frequency components, but also does not cause the difficulty of predicting high-frequency components to an unacceptable level due to excessive extraction of low-frequency components. In this paper, the optimal frequency is solved by minimizing the square of the difference that the correlation between low-frequency components and raw data is subtracted from the correlation between high-frequency components and raw data, which can be regarded as an optimization problem. The specific formula is given in Eq. (7).

$$\begin{aligned} \min F(f) &= [L(f) - H(f)]^2 \\ \text{s.t. } f &\in \left[0, \frac{N}{2}\right] \end{aligned} \quad (7)$$

Among them, $F(f)$ is an objective function. When the objective function reaches the minimum value, the correlation between low-frequency components and raw data and the correlation between high-frequency components and raw data reach an optimal balance. $L(f)$ is the correlation between low-frequency components and raw data, $H(f)$ is the correlation between high frequency components and raw data, and N is the total number of sampling frequencies.

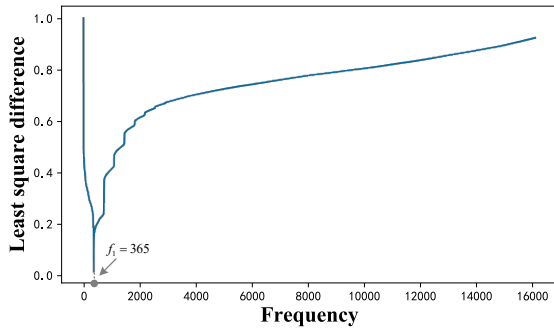


Fig. 8. The graph of the squared difference before weighting

Fig. 8 is a graph of the obtained square of the difference that the correlation between low-frequency components and raw data is subtracted from the correlation between high-frequency components and raw data. It can be seen from the Fig. 8 that when the frequency demarcation point f_1 is 365, the correlation between low-frequency components and raw data and the correlation between high-frequency components and raw data reach a balance. However, due to the strong regularity and high prediction accuracy of low-frequency components, this article first hopes that the proportion of low-frequency components is high. When the frequency value continues to increase, the correlation between the low-frequency components and raw data can be improved. However, when the correlation between the low-frequency components and raw data is basically unchanged, the prediction accuracy of low-frequency components basically reaches the maximum value. At this time, the accuracy of final prediction result mainly depends on high-frequency components. Therefore, in order to give priority to low-frequency components, the frequency value is continuously increased. This article adds weight values to the objective function in Eq. (7). By multiplying the correlation between low-frequency components and raw data by a low weight value and multiplying the correlation between high-frequency components and raw data by a high weight value. In this way, the design idea of giving priority to low-frequency components is achieved. The new objective function is shown by Eq. (8). This paper chooses $\alpha = 0.173$, $\beta = 0.827$, and obtains the frequency demarcation point $f_2 = 1825$.

$$\min F(f) = [\alpha L(f) - \beta H(f)]^2 \quad (8)$$

$$s.t. \quad f \in \left[0, \frac{N}{2}\right]$$

Where α is the weight of the correlation between the low frequency component and the original data, and β is the weight of the correlation between the high frequency component and the original data.

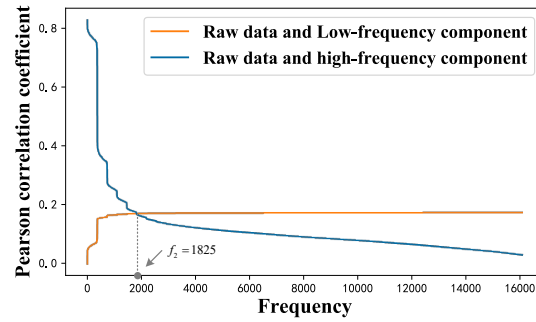


Fig. 9. Correlation between decomposition components and raw data after weighting

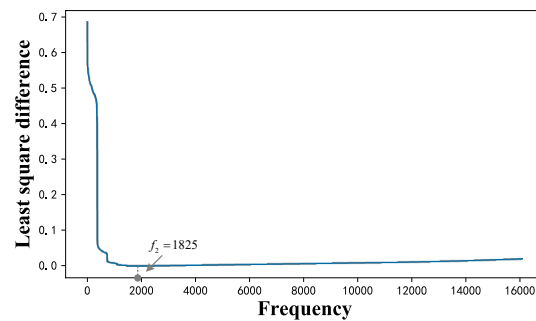


Fig. 10. The graph of the squared difference after weighting

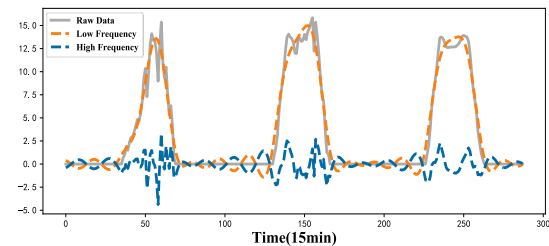


Fig. 11. Optimal frequency decomposition result

Fig. 9 shows correlation between decomposition components and raw data after weighting. Fig. 10 shows the square of the difference that the correlation between low-frequency components and raw data is subtracted from the correlation between high-frequency components and raw data after weighting. It can be seen that after f_2 , as the frequency band increases, the correlation between low-frequency components and raw data does not increase significantly, while the correlation between high-frequency components still maintains a downward trend in Fig. 9. Therefore, f_2 is the optimal frequency demarcation point f_o . Fig. 11 shows the decomposition results at frequency demarcation point f_o .

TABLE II. COMPARISON OF R OF LOW FREQUENCY COMPONENTS AT DIFFERENT FREQUENCIES

| Component | R | | | | | |
|----------------|--------|--------|--------|--------|---------|---------|
| | 365 | 730 | 1092 | 1458 | 1825 | 2185 |
| Low frequency | 0.9243 | 0.9654 | 0.9792 | 0.9994 | 0.9997 | 0.9998 |
| High frequency | 0.6722 | 0.6584 | 0.4783 | 0.2947 | -0.1446 | -0.1876 |

IV. CASE STUDY

4.1 Simulation data and simulation platform

The data used for the simulation in this section are historical weather data and historical power with 15 min time resolution from 0:00 on January 1 in 2017 to 23:45 on December 31 in 2017 in Ningxia PV Power Station and Jilin PV Power Station in China. This article uses the data from 0:00 on January 1 in 2017 to 23:45 on November 30 in 2017 as training set, and the data from 0:00 on December 1 in 2017 to 23:45 on December 31 in 2017 as testing set. The time scale of input data is 24 hours, and the time scale of output data is 1 hour.

We use Python 3.6.1 with Tensorflow and scikit-learn to perform all the simulations.

4.2 Data processing

During model training, to eliminate the difference in magnitude between each dimension data, the samples of input data will be normalized. The range of values of all samples is converted to [0, 1], which avoids large differences in sample magnitude leads to large network prediction errors. Its formula is shown in (9):

$$M^* = \frac{M - M_{\min}}{M_{\max} - M_{\min}} \quad (9)$$

4.3 Performance criterion

In order to evaluate the performance of the prediction model, we employ two effective error indexes that are Mean Absolute Percentage Error (MAPE) and Root Mean Squared Error (RMSE). Under the same set of training data, the smaller MAPE and RMSE, together with the higher R, and the better the prediction model effect. The mathematical formulas for the two error indexes are shown in (10) and (11):

$$MAPE = \frac{1}{N} \sum_{t=1}^N \left| \frac{y_t - \hat{y}_t}{y_t} \right| \quad (10)$$

$$RMSE = \sqrt{\frac{\sum_{t=1}^N (y_t - \hat{y}_t)^2}{N}} \quad (11)$$

4.4 Calculation of forecast uncertainty

Uncertainty is a major problem in all photovoltaic power prediction models. Various uncertain factors affecting grid operation can be divided into three factors: (1) due to input, that is measurement error related to weather variables; (2) due to the inherent randomness of the basic physical process; (3) Inherent to the model structure, namely the selected parameters and the training data set used for the purpose of model building. This article refers to the literatures [30-31], and adopts the method of quantifying solar photovoltaic power generation forecast in the form of *PI*.

The *PI* with a predefined confidence level α % is the interval between the upper and lower limits of predicted power generation at time t , $t \in [1, 24]$ of day d

$\left[\hat{P}_{test_j}^{lower}(t, d), \hat{P}_{test_j}^{upper}(t, d) \right]$, so that the actual “unknown”

value $P_{test_j}(t, d)$, of the j -th test pattern at time t of day d , falls within the interval, and its probability is equal to α %:

$$PI^\alpha = \left[\hat{P}_{test_j}^{lower}(t, d), \hat{P}_{test_j}^{upper}(t, d) \right], \quad (12)$$

$$Prob\left(\hat{P}_{test_j}^{lower}(t, d) \leq P_{test_j}(t, d) \leq \hat{P}_{test_j}^{upper}(t, d)\right) = \alpha\%$$

Referring to literatures [30-31], this article uses two performance indicators to evaluate the forecast uncertainty, namely *PI* coverage probability (*PICP*) and *PI* width (*PIW*). The goal of a *PI* with a confidence level of α % is to cover at least α % with as small a width as possible. This section uses the data from 0:00 on January 1 in 2017 to 23:45 on November 30 in 2017 as training set, and the data from 0:00 on December 1 in 2017 to 23:45 on December 31 in 2017 as testing set in Ningxia PV Power Station and Jilin PV Power Station in China. The time scale of input data is 24 hours, and the time scale of output data is 1 hour. Table III reports the *PI*s performances obtained by the proposed approach in terms of *PICP* and *PIW*. From the results in Table III, it can be seen that the coverage of *PI* is higher than the target coverage level of 0.8, and the width of *PI* is also is also smaller. To a certain extent, it can be seen that the FFD prediction model proposed in this paper can reduce forecast uncertainty.

TABLE III PIS PERFORMANCES OBTAINED BY FDD PREDICTION MODEL ON THE TEST DATASET, FOR $\alpha=80\%$ TARGET CONFIDENCE LEVEL.

| Prediction Intervals for | Performance | |
|--------------------------|---------------|--------|
| | $\alpha=80\%$ | |
| Direct | 0.61196 | 0.4256 |
| DWT | 0.6092 | 0.1889 |
| VMD | 0.7324 | 0.1051 |
| FDD | 0.8164 | 0.1106 |

4.5 Performance analysis of frequency-domain decomposition forecasting model on different weather types.

This paper establishes frequency-Domain decomposition forecasting model of PV power on sunny day, cloudy day, light rainy day and heavy rainy day. In this part, two different data sets, Ningxia Power Station and Jilin Power Station, are used to compare the performance of frequency-Domain decomposition forecasting model of different weather types. In this section, frequency-domain decomposition forecasting model with predicting 1 hour time scale is compared with other VMD, DWT and Direct models, and the prediction model is unified using the CNN model.

4.5.1 Comparison analysis of sunny days

Fig. 12(a) shows actual and forecasted PV power on sunny day using dataset of Ningxia Power Station. Fig. 13(a) shows Error distribution curves of direct prediction model and frequency decomposition prediction model on sunny day using dataset of Ningxia Power Station. Fig. 14(a) shows Linear regression graph of direct prediction model and frequency decomposition prediction model on sunny day using dataset of Ningxia Power Station. Fig. 15(a) shows The generation of forecast error graph of different sunny days' decomposition prediction models using the dataset of Ningxia Power Station.

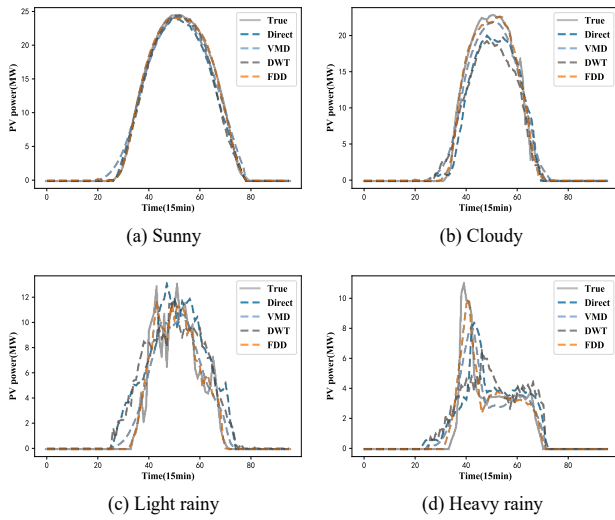


Fig. 12. Actual and forecasted PV power on four different weather types using dataset of Ningxia Power Station.

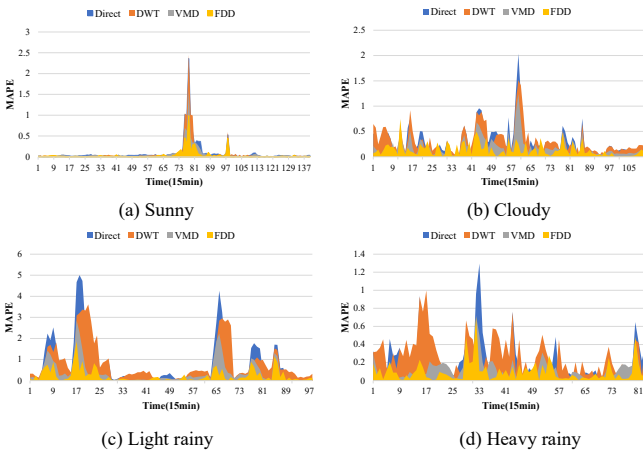


Fig. 13. Error distribution curves of different decomposition prediction models on four different weather types using dataset of Ningxia Power Station.

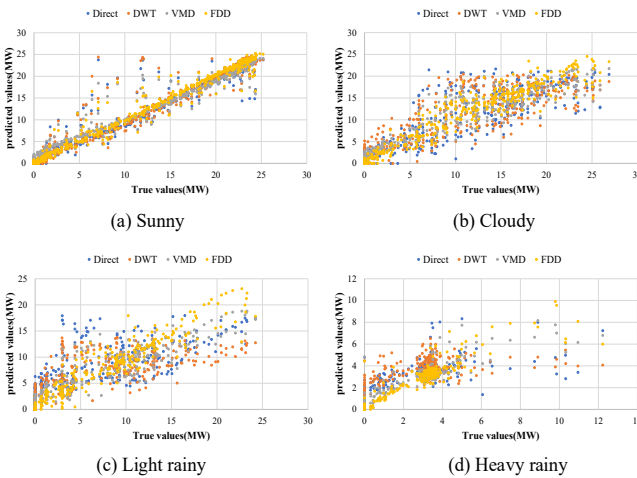


Fig. 14. Linear regression graph of different decomposition prediction models on four different weather types using dataset of Ningxia Power Station.

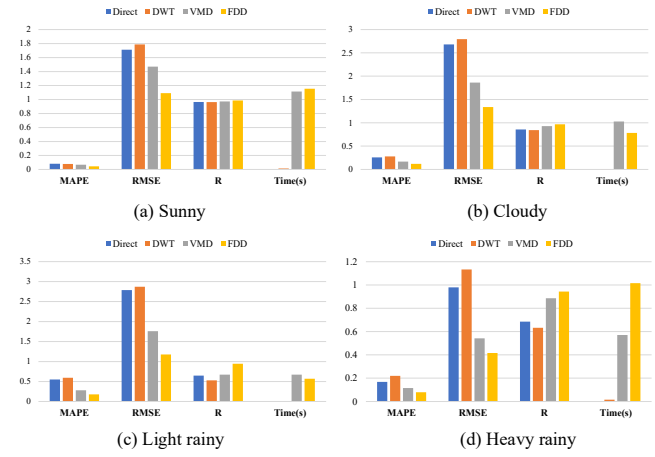


Fig. 15. The generation of forecast error graph of different decomposition prediction models on four different weather types using the dataset of Ningxia Power Station.

Table IV and Table V show the performance comparison of the sunny weather prediction models for different data sets. Taking Ningxia Power Station as an example, in sunny days, compared with DWT, VMD and direct prediction models, the MAPE accuracy of the FDD model proposed in this paper is increased by 42.05%, 32.94% and 44.59% respectively, and the RMSE accuracy is increased by 38.91%, 25.72% and 36.20% respectively, and the R is increased by 2.24%, 1.41% and 2.21% respectively. The performance comparison result of Jilin Power Station shown in Table V is similar to Ningxia Power Station. This is mainly because on a sunny day, since the sky has almost no shadow and the physical state of the atmosphere is relatively stable, the photovoltaic power curve on a sunny day is smooth with small fluctuations. Therefore, the frequency domain decomposition prediction model proposed in this paper will not bring about a very significant improvement in prediction performance.

TABLE IV. THE PERFORMANCE COMPARISON OF DIFFERENT SUNNY DAYS' DECOMPOSITION PREDICTION MODELS USING THE DATASET OF NINGXIA POWER STATION

| Model | Performance | | | |
|--------|-------------|--------|--------|---------|
| | MAPE | RMSE | R | Time(s) |
| Direct | 0.0823 | 1.7118 | 0.9648 | / |
| DWT | 0.0787 | 1.7876 | 0.9629 | 0.01395 |
| VMD | 0.0680 | 1.4703 | 0.9724 | 1.1139 |
| FDD | 0.0456 | 1.092 | 0.9862 | 1.1543 |

TABLE V. THE PERFORMANCE COMPARISON OF DIFFERENT SUNNY DAYS' DECOMPOSITION PREDICTION MODELS USING THE DATASET OF JILIN POWER STATION

| Model | Performance | | | |
|--------|-------------|--------|---------|---------|
| | MAPE | RMSE | R | Time(s) |
| Direct | 0.1108 | 1.6144 | 0.9309 | / |
| DWT | 0.1225 | 1.7453 | 0.9217 | 0.0249 |
| VMD | 0.1010 | 1.2483 | 94.9751 | 0.6226 |
| FDD | 0.0697 | 0.7684 | 0.9837 | 0.5348 |

4.5.2 Comparison analysis of cloudy days

Fig. 12(b) shows actual and forecasted PV power on cloudy day using dataset of Ningxia Power Station. Fig. 13(b)

shows Error distribution curves of direct prediction model and frequency decomposition prediction model on cloudy day using dataset of Ningxia Power Station. Fig. 14(b) shows Linear regression graph of direct prediction model and frequency decomposition prediction model on cloudy day using dataset of Ningxia Power Station. Fig. 15(b) shows The generation of forecast error graph of different cloudy days' decomposition prediction models using the dataset of Ningxia Power Station. Table VI and Table VII show the performance comparison of the cloudy weather prediction models for different data sets. Taking Ningxia Power Station as an example, in cloudy days, compared with DWT, VMD and direct prediction models, the MAPE accuracy of the FDD model proposed in this paper is increased by 57.42%, 29.64% and 53.86% respectively, and the RMSE accuracy is increased by 52.16%, 28.22% and 50.10% respectively, the R is increased by 14.77%, 4.16% and 12.94% respectively. The performance comparison result of Jilin Power Station shown in Table VII is similar to Ningxia Power Station. These changes have slightly reduced the accuracy of photovoltaic power generation forecasts. The frequency domain decomposition prediction model proposed in this paper can improve the prediction performance of the model under cloudy conditions.

TABLE VI. THE PERFORMANCE COMPARISON OF DIFFERENT CLOUDY DAYS' DECOMPOSITION PREDICTION MODELS USING THE DATASET OF NINGXIA POWER STATION

| Model | Performance | | | |
|--------|-------------|--------|--------|---------|
| | MAPE | RMSE | R | Time(s) |
| Direct | 0.2577 | 2.6796 | 0.8569 | / |
| DWT | 0.2793 | 2.7951 | 0.8432 | 0.0060 |
| VMD | 0.1690 | 1.8628 | 0.9291 | 1.0276 |
| FDD | 0.1189 | 1.3371 | 0.9678 | 0.7834 |

TABLE VII. THE PERFORMANCE COMPARISON OF DIFFERENT CLOUDY DAYS' DECOMPOSITION PREDICTION MODELS USING THE DATASET OF JILIN POWER STATION

| Model | Performance | | | |
|--------|-------------|--------|--------|---------|
| | MAPE | RMSE | R | Time(s) |
| Direct | 0.1229 | 1.6716 | 0.9276 | / |
| DWT | 0.1093 | 1.2888 | 0.9657 | 0.0293 |
| VMD | 0.1183 | 1.4793 | 0.9442 | 2.1763 |
| FDD | 0.0636 | 0.8428 | 0.9856 | 1.6252 |

4.5.3 Comparison analysis of light rainy days

Fig. 12(c) shows actual and forecasted PV power on light rainy day using dataset of Ningxia Power Station. Fig. 13(c) shows Error distribution curves of direct prediction model and frequency decomposition prediction model on light rainy day using dataset of Ningxia Power Station. Fig. 14(c) shows Linear regression graph of direct prediction model and frequency decomposition prediction model on light rainy day using dataset of Ningxia Power Station. Fig. 15(c) shows The generation of forecast error graph of different light rainy days' decomposition prediction models using the dataset of Ningxia Power Station. Table VIII and Table IX show the performance comparison of the light rainy weather prediction models for different data sets. Taking Ningxia Power Station as an example, in light rainy days, compared with DWT, VMD and direct prediction models, the MAPE accuracy of the FDD model proposed in this paper is increased by 64.07%, 31.21% and 52.97%, respectively, and the RMSE accuracy is 63.30%, 23.19% and 57.56% respectively, the R increased by 49.02%, 6.43% and 37.69% respectively. The performance comparison result of Jilin Power Station shown in Table XI is similar to Ningxia Power Station. In heavy rainy days, the irradiance attenuation is serious, and the photovoltaic power curve of heavy rainy days includes more spikes and nonlinear fluctuation components, which makes the accuracy of photovoltaic power generation prediction poor. The frequency domain decomposition prediction model

model proposed in this paper is increased by 70.11%, 36.79% and 67.77% respectively, and the RMSE accuracy is increased by 59.05%, 33.22% and 57.79% respectively, the R is increased by 77.84%, 40.25% and 45.64% respectively. The performance comparison result of Jilin Power Station shown in Table IX is similar to Ningxia Power Station. Due to changes in the physical state of the atmosphere during light rainy days, the photovoltaic power curves of light rainy days may include spikes and nonlinear fluctuation components. The accuracy of photovoltaic power generation forecasts is reduced. The frequency domain decomposition prediction model proposed in this paper can improve the prediction performance of the model under light rainy days.

TABLE VIII. THE PERFORMANCE COMPARISON OF DIFFERENT LIGHT RAINY DAYS' DECOMPOSITION PREDICTION MODELS USING THE DATASET OF NINGXIA POWER STATION

| Model | Performance | | | |
|--------|-------------|--------|--------|---------|
| | MAPE | RMSE | R | Time(s) |
| Direct | 0.5517 | 2.7858 | 0.6480 | / |
| DWT | 0.5949 | 2.8711 | 0.5307 | 0.0096 |
| VMD | 0.2813 | 1.7607 | 0.6729 | 0.6729 |
| FDD | 0.1778 | 1.1757 | 0.9438 | 0.5701 |

TABLE IX. THE PERFORMANCE COMPARISON OF DIFFERENT LIGHT RAINY DAYS' DECOMPOSITION PREDICTION MODELS USING THE DATASET OF JILIN POWER STATION

| Model | Performance | | | |
|--------|-------------|--------|--------|---------|
| | MAPE | RMSE | R | Time(s) |
| Direct | 0.3743 | 2.4740 | 0.6560 | / |
| DWT | 0.4500 | 2.6674 | 0.5879 | 0.1249 |
| VMD | 0.2629 | 1.6366 | 0.8597 | 0.8904 |
| FDD | 0.2159 | 1.2539 | 0.9322 | 0.4686 |

4.5.4 Comparison analysis of heavy rainy days

Fig. 12(d) shows actual and forecasted PV power on heavy rainy day using dataset of Ningxia Power Station. Fig. 13(d) shows Error distribution curves of direct prediction model and frequency decomposition prediction model on heavy rainy day using dataset of Ningxia Power Station. Fig. 14(d) shows Linear regression graph of direct prediction model and frequency decomposition prediction model on heavy rainy day using dataset of Ningxia Power Station. Fig. 15(d) shows The generation of forecast error graph of different heavy rainy days' decomposition prediction models using the dataset of Ningxia Power Station. Table X and Table XI show the performance comparison of the heavy rainy weather prediction models for different data sets. Taking Ningxia Power Station as an example, in heavy rainy days, compared with DWT, VMD and direct prediction models, the MAPE accuracy of the FDD model proposed in this paper is increased by 64.07%, 31.21% and 52.97%, respectively, and the RMSE accuracy is 63.30%, 23.19% and 57.56% respectively, the R increased by 49.02%, 6.43% and 37.69% respectively. The performance comparison result of Jilin Power Station shown in Table XI is similar to Ningxia Power Station. In heavy rainy days, the irradiance attenuation is serious, and the photovoltaic power curve of heavy rainy days includes more spikes and nonlinear fluctuation components, which makes the accuracy of photovoltaic power generation prediction poor. The frequency domain decomposition prediction model

proposed in this paper can improve the prediction performance of the model under heavy rainy days.

TABLE X. THE PERFORMANCE COMPARISON OF DIFFERENT HEAVY RAINY DAYS' DECOMPOSITION PREDICTION MODELS USING THE DATASET OF NINGXIA POWER STATION

| Model | Performance | | | |
|--------|-------------|--------|--------|---------|
| | MAPE | RMSE | R | Time(s) |
| Direct | 0.1682 | 0.9798 | 0.6850 | / |
| DWT | 0.2202 | 1.1330 | 0.6329 | 0.0157 |
| VMD | 0.1150 | 0.5414 | 0.8862 | 0.5702 |
| FDD | 0.0791 | 0.4158 | 0.9432 | 1.0157 |

TABLE XI. THE PERFORMANCE COMPARISON OF DIFFERENT HEAVY RAINY DAYS' DECOMPOSITION PREDICTION MODELS USING THE DATASET OF JILIN POWER STATION

| Model | Performance | | | |
|--------|-------------|--------|--------|---------|
| | MAPE | RMSE | R | Time(s) |
| Direct | 0.5307 | 1.6808 | 0.3401 | / |
| DWT | 0.8167 | 1.8750 | 0.1171 | 0.01 |
| VMD | 0.2793 | 1.0161 | 0.7757 | 0.6718 |
| FDD | 0.2388 | 0.8142 | 0.8849 | 0.2655 |

4.6 Comparison and analysis of the performance of different PV forecasting models

This paper uses the unified frequency domain decomposition model to compare the CNN prediction model with other prediction models. Fig. 16 and Fig. 17 show the MAPE, RMSE, R and time of different prediction models for sunny, cloudy, light rainy and heavy rainy days using the data of Ningxia and Jilin power stations. Compared with other prediction models such as BP Neural Network, RNN and LSTM, the prediction accuracy of the CNN prediction model is higher, and due to weight sharing, the model training time is greatly shortened. Taking Ningxia power station data on heavy rainy day as an example, after decomposing uniformly using the FDD model proposed in this paper, compared with BP neural network, RNN and LSTM models, the MAPE accuracy of CNN prediction model is improved by 14.02%, 23.64% and 46.22%. And compared with RNN and LSTM models, the train time efficiency of CNN prediction model is improved by 85.63% and 87.68%. Although the training time of BP neural network is a little less than CNN, CNN has better prediction accuracy. Generally speaking, compared with other prediction models such as BP Neural Network, RNN and LSTM, the prediction accuracy of the CNN prediction model is higher, and due to weight sharing, the model training time is greatly shortened. The results fully show that the CNN model proposed in this paper improves the prediction accuracy and time efficiency.

4.7 Simulation Discussion

It can be seen from the above results that in the four weather types, the proposed frequency domain decomposition method improves the prediction accuracy. Although the high-frequency components are more volatile after the lack of low-frequency components, this may cause the prediction accuracy of the high-frequency components to decrease. However, the method of selecting the best frequency division point

proposed in this paper not only increases the proportion of low-frequency components in the original data, but also balances the difficulty of predicting high-frequency components to a certain extent. Therefore, after adding and reconstructing low-frequency and high-frequency components, the accuracy of the final result is usually improved.

In addition, the results also show that the training time for CNN prediction is reduced. This is because the weight sharing technology enables CNN to reduce the parameters to be estimated, thereby shortening the training time. And CNN can perform feature extraction on data, which has good robustness. Therefore, the CNN model can improve the accuracy and efficiency of the ultra-short-term prediction of photovoltaic power generation.

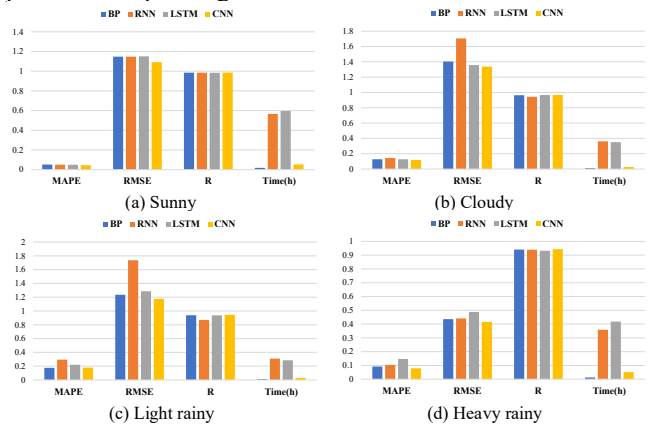


Fig. 16. The performance of different prediction models on four different weather types using the dataset of Ningxia Power Station.

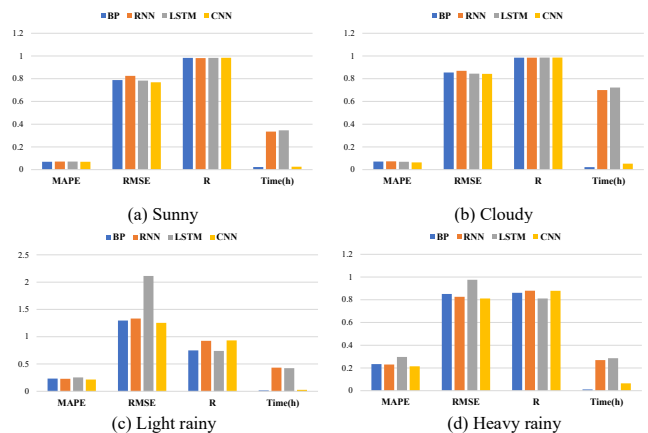


Fig. 17. The performance of different prediction models on four different weather types using the dataset of Jilin Power Station.

V. CONCLUSION

To overcome the shortcomings that there is currently no effective method to support the rationality of the frequency domain decomposition results, this paper proposes an ultra-short-term prediction model of PV power based on optimal frequency-domain decomposition and deep learning. First, the amplitude and phase of each frequency sine wave is obtained by fast Fourier decomposition. As the frequency demarcation point is different, the correlation between the decomposition component and the original data is analyzed. By minimizing the square of the difference that the correlation between low-frequency components and raw data is subtracted from the correlation between high-frequency components and raw data,

the optimal frequency demarcation points for decomposition components are obtained. Then convolutional neural network is used to predict low-frequency component and high-frequency component, and final prediction result is obtained by addition reconstruction.

For the decomposition model proposed in this article, by minimizing the square of the difference that the correlation between low-frequency components and raw data is subtracted from the correlation between high-frequency components and raw data, the optimal frequency demarcation points for decomposition components are obtained, and the PV power is decomposed into the low frequency Components and high-frequency components. The low-frequency component represents the regular part of photovoltaic power generation, which shows its trend characteristics, while the high-frequency component represents the randomness of photovoltaic power generation, which shows its fluctuation characteristics affected by other factors such as weather. This method supports the rationality of the decomposition results and solves the problem that the current decomposition model only uses the direct decomposition method, and the decomposition components have no physical meaning. Taking Ningxia power station data as an example, compared with discrete wavelet transform, variational mode decomposition and direct prediction models, the MAPE accuracy of the proposed frequency domain decomposition prediction model is improved by 42.05%, 32.94% and 44.59% respectively on sunny day, is improved by 57.42%, 29.64% and 53.86% on cloudy day, is improved by 70.11%, 36.79% and 67.77% on light rainy day, and is improved by 64.07%, 31.21% and 52.97% on heavy rainy day. The RMSE accuracy of the proposed frequency domain decomposition prediction model is improved by 38.91%, 25.72% and 36.20% respectively on sunny day, is improved by 52.16%, 28.22% and 50.10% on cloudy day, is improved by 59.05%, 33.22% and 57.79% on light rainy day, and is improved by 63.30%, 23.19% and 57.56% on heavy rainy day. The R accuracy of the proposed frequency domain decomposition prediction model is improved by 2.24%, 1.41% and 2.21% respectively on sunny day, is improved by 14.77%, 4.16% and 12.94% on cloudy day, is improved by 77.84%, 40.25% and 45.64% on light rainy day, and is improved by 49.02%, 6.43% and 37.69% on heavy rainy day. The results fully show that the FDD method in this paper improves the consistency of experimentally observed data and forecast data.

For the prediction model proposed, CNN is not only successfully applied to image processing, but also used to solve one-dimensional data classification and regression problems. CNN reduces the parameters to be estimated due to the weight sharing technology, thereby shortening the training time for prediction. And CNN can perform feature extraction on the data, which has good robustness. Therefore, this article is dedicated to the reasonable application of CNN model to improve the accuracy and efficiency of ultra-short-term prediction of photovoltaic power. Taking Ningxia power station data on heavy rainy day as an example, after decomposing uniformly using the FDD model proposed in this paper, compared with BP neural network, RNN and LSTM models, the MAPE accuracy of CNN prediction model is improved by 14.02%, 23.64% and 46.22%. And compared with RNN and LSTM models, the train time efficiency of CNN prediction model is improved by 85.63% and 87.68%.

Although the training time of BP neural network is a little less than CNN, CNN has better prediction accuracy. Generally speaking, compared with other prediction models such as BP Neural Network, RNN and LSTM, the prediction accuracy of the CNN prediction model is higher, and due to weight sharing, the model training time is greatly shortened. The results fully show that the CNN model proposed in this paper improves the prediction accuracy and time efficiency.

The above results show that the frequency domain decomposition prediction model has high superiority in the accuracy and time efficiency of ultra-short-term prediction of photovoltaic power, especially in extreme weather conditions [32]. The ultra-short-term prediction of photovoltaic power based on deep learning proposed in this paper has very high application prospects in the area of demand response aggregator [33], such as aggregated capacity forecasting [34], automatic demand response strategy [35], day-ahead optimal bidding and scheduling [36].

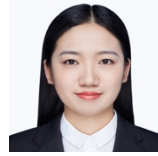
REFERENCES

- [1] K. Li, F. Wang, Z. Mi, M. Fotuhi-Firuzabad, N. Dui, and T. Wang, "Capacity and output power estimation approach of individual behind-the-meter distributed photovoltaic system for demand response baseline estimation," *Appl. Energy*, vol. 253, pp. 113595, Nov. 2019.
- [2] F. Wang, Z. Zhen, B. Wang, and Z. Mi, "Comparative study on KNN and SVM based weather classification models for day ahead short term solar PV power forecasting," *Appl. Sci.-Basel.*, vol. 8, no. 1, Jan. 2018.
- [3] F. Wang, Z. Zhen, C. Liu, Z. Mi, M. Shafie-Khah, and JPS. Catalao, "Time-section fusion pattern classification based day-ahead solar irradiance ensemble forecasting model using mutual iterative optimization," *Energies*, vol. 11, no. 1, Jan. 2018.
- [4] Z. Zhen, S. Pang, F. Wang, K. Li, Z. Li, H. Ren, M. Shafie-Khah, and JPS. Catalao., "Pattern classification and PSO optimal weights based sky images cloud motion speed calculation method for solar PV power forecasting," *IEEE Trans. Ind. Appl.*, vol. 55, no. 4, pp. 3331-3342, Jul./Aug. 2019.
- [5] F. Wang, Z. Zhen, C. Liu, Z. Mi, SM. Hodge, M. Shafie-Khah, and JPS. Catalao, "Image phase shift invariance based cloud motion displacement vector calculation method for ultra-short-term solar PV power forecasting," *Energy Convers. Manage.*, vol. 157, pp. 123-135, Feb. 2018.
- [6] J. Kamadinata, T. Ken, and T. Suwa, "Sky image-based solar irradiance prediction methodologies using artificial neural networks," *Renew. Energy*, vol. 134, pp. 837-845, Apr. 2019.
- [7] F. Wang, Z. Zhen, Z. Mi, H. Sun, S. Su, and G. Yang, "Solar irradiance feature extraction and support vector machines based weather status pattern recognition model for short-term photovoltaic power forecasting," *Energy Build.*, vol. 86, pp. 427-438, Jan. 2015.
- [8] F. Wang, Z. Mi, S. Su, and H. Zhao, "Short-term solar irradiance forecasting model based on artificial neural network using statistical feature parameters," *Energies*, vol. 5, no. 5, pp. 1355-1370, May. 2012.
- [9] H. Yang, C. Huang, Y. Huang, and Y. Pai, "A weather-based hybrid method for 1-day ahead hourly forecasting of PV power output," *IEEE Trans. Sustain. Energy*, vol. 5, no. 3, pp. 917-926, Jul. 2014.
- [10] J. Shi, W. Lee, Y. Liu, Y. Yang, and P. Wang, "Forecasting power output of photovoltaic systems based on weather classification and support vector machines," *IEEE Trans. Ind. Appl.*, vol. 48, no. 3, pp. 1064-1069, May./Jun. 2012.
- [11] P. Lin, Z. Peng, Y. Lai, S. Cheng, Z. Chen, and L. Wu, "Short-term power prediction for photovoltaic power plants using a hybrid improved Kmeans-GRA-Elman model based on multivariate meteorological factors and historical power datasets," *Energy Convers. Manage.*, vol. 177, pp. 704-717, Dec. 2018.
- [12] H. Zhang, L. Cheng, T. Ding, K. Cheung, Z. Liang, Z. Wei, and G. Sun, "Hybrid method for short-term photovoltaic power forecasting based on deep convolutional neural network," *IET Gener. Transm. Distrib.*, vol. 12, no. 20, pp. 4557-4567, Nov. 2018.
- [13] V. Kushwaha, and N. Pindoriya, "A SARIMA-RVFL hybrid model assisted by wavelet decomposition for very short-term solar PV power generation forecast," *Renew. Energy*, vol. 140, pp. 124-139, Sep. 2019.
- [14] W. Zhang, H. Dang, and R. Simoes, "A new solar power output prediction based on hybrid forecast engine and decomposition model," *ISA Trans.*, vol. 81, pp. 105-120, Oct. 2018.

- [15] M. Lima, P. Carvalho, L. Fernandez-Ramirez, A. Braga., "Improving solar forecasting using Deep Learning and Portfolio Theory integration," *Energy*, vol. 195, pp. 117016, Mar. 2020.
- [16] F. Wang, Z. Zhen, C. Liu, Z. Mi, B.M. Hodge, M. Shafie-khah, and JPS. Catalao, "Image phase shift invariance based cloud motion displacement vector calculation method for ultra-short-term solar PV power forecasting," *Energy Convers. Manage.*, vol. 157, pp. 123-135, Feb. 2018.
- [17] M. Madhjarasan, "Accurate prediction of different forecast horizons wind speed using a recursive radial basis function neural network," *Prot Control. Mod. Power Syst.*, vol. 5, no. 22, 2020.
- [18] J. Liu, W. Fang, X. Zhang, and C. Yang, "An improved photovoltaic power forecasting model with the assistance of aerosol index data," *IEEE Trans. Sustain. Energy*, vol. 6, no. 2, pp. 434-442, Apr. 2015.
- [19] M. Bozorg, A. Bracale, P. Caramia, et al, "Bayesian bootstrap quantile regression for probabilistic photovoltaic power forecasting," *Prot Control Mod. Power Syst.*, vol.5, no. 21, 2020.
- [20] Z. Zhen, F. Wang, Y. Sun, C. Liu, B. Wang, and J. Lu, "SVM based cloud classification model using total sky images for PV power forecasting," 2015 IEEE PES Innovative Smart Grid Technologies, Washington, DC, USA, 18-20 Feb. 2015.
- [21] Qing X, and Niu Y, "Hourly day-ahead solar irradiance prediction using weather forecasts by LSTM," *Energy*, vol. 148, pp. 461-468, Apr. 2018.
- [22] F. Wang, Z. Xuan, Z. Zhen, K. Li, T. Wang, and M. Shi, "A day-ahead PV power forecasting method based on LSTM-RNN model and time correlation modification under partial daily pattern prediction framework," *Energy Convers. Manage.*, vol. 212, pp. 112766, May. 2020.
- [23] Q. Huang, and S. Wei, "Improved quantile convolutional neural network with two-stage training for daily-ahead probabilistic forecasting of photovoltaic power," *Energy Convers. Manage.*, vol. 220, pp. 113085, Sep. 2020.
- [24] M. Alam, S. Rehman, L. Al-Hadhrami, and J. Meyer, "Extraction of the inherent nature of wind speed using wavelets and FFT," *Energy Sustain. Dev.*, vol. 22, pp. 34-47, Oct. 2014.
- [25] M. Yang, and X. Huang, "Ultra-short-term prediction of photovoltaic power based on periodic extraction of PV energy and LSH algorithm," *IEEE Access*, vol. 6, pp. 51200-51205, 2018.
- [26] M. Yang, and X. Huang, "An evaluation method of the photovoltaic power prediction quality," *Math. Probl. Eng.*, vol. 2018, 2018.
- [27] T. Kim, and S. Cho, "Predicting residential energy consumption using CNN-LSTM neural networks," *Energy*, vol. 182, pp. 72-81, Sep. 2019.
- [28] F. Wang, Y. Yu, Z. Zhang, J. Li, Z. Zhen, and K. Li, "Wavelet decomposition and convolutional LSTM networks based improved deep learning model for solar irradiance forecasting," *Appl. Sci.-Basel*, vol. 8, no. 8, Aug. 2018.
- [29] F. Wang, Z. Zhang, C. Liu, Y. Yu, S. Pang, N. Duic, M. Shafie-Khah, and JPS. Catalao., "Generative adversarial networks and convolutional neural networks based weather classification model for day ahead short-term photovoltaic power forecasting," *Energy Convers. Manage.*, vol. 181, pp. 443-462, Feb. 2019.
- [30] S. Al-Dahidi, O. Ayadi, M. Alrbai, and J. Adee, "Ensemble approach of optimized artificial neural networks for solar photovoltaic power prediction," *IEEE Access*, vol. 7, pp. 81741-81758, 2019.
- [31] R. Ahmed, V. Sreeram, Y. Mishra, and M.D. Arif, "A review and evaluation of the state-of-the-art in PV solar power forecasting: Techniques and optimization," *Renew. Sust. Energ. Rev.*, vol. 124, pp. 109792, May. 2020.
- [32] L. Hu et al., "Ultra-Short-Term Solar PV Power Forecasting Method Based on Frequency-Domain Decomposition and Deep Learning," 2020 IEEE Industry Applications Society Annual Meeting, Detroit, MI, USA, 2020, pp. 1-8, doi: 10.1109/IAS44978.2020.9334889.
- [33] X. Lu, K. Li, H. Xu, F. Wang, Z. Zhou, and Y. Zhang, "Fundamentals and business model for resource aggregator of demand response in electricity markets," *Energy*, vol. 204, no. 117885, May 2020.
- [34] F. Wang, B. Xiang, K. Li, X. Ge, H. Lu, J. Lai, and P. Dehghanian, "Smart households' aggregated capacity forecasting for load aggregators under incentive-based demand response programs," *IEEE Trans. Ind. Appl.*, vol. 56, no. 2, pp. 1086-1097, Mar.-Apr. 2020.
- [35] Q. Chen, F. Wang, B.M. Hodge, J. Zhang, Z. Li, M. Shafie-khah, and J. P. S. Catalão, "Dynamic price vector formation model-based automatic demand response strategy for PV-assisted EV charging stations," *IEEE Trans. Smart Grid*, vol. 8, no. 6, pp. 2903-2915, Nov. 2017.
- [36] F. Wang, X. Ge, P. Yang, K. Li, Z. Mi, P. Siano, and N. Duić, "Day-ahead optimal bidding and scheduling strategies for DER aggregator considering responsive uncertainty under real-time pricing," *Energy*, vol. 213, no. 118765, Dec. 2020.



Jichuan Yan (Student Member, IEEE) received the B.S. degree in Electrical Engineering from Zhejiang University of Technology, Hangzhou, China, in 2020. He is currently working toward the M.S. degree in the Department of Electrical Engineering, North China Electric Power University, Baoding, China. His research interests include demand response, power forecasting and electricity market.



Lin Hu received the B.S. degree in Electrical Engineering and Automation from Hebei Normal University, Shijiazhuang, China, in 2018. She is currently working toward the M.S. degree in the Department of Electrical Engineering, North China Electric Power University, Baoding, China. Her research interests include solar PV power and net load forecasting.



Zhao Zhen received the B.S. degree and Ph.D. degrees in Electrical Engineering from North China Electric Power University (NCEPU), Baoding, China, in 2012, 2018, respectively. Currently, he is an assistant professor with the Department of Electrical Engineering at NCEPU, Baoding, China and also a postdoc researcher with the department of electrical engineering at Tsinghua University. His research interests include solar irradiance and PV power forecasting, wind speed and power forecasting.



Fei Wang (M'09-SM'17) received the B.S. degree from Hebei University, Baoding, China in 1993, the M.S. and Ph.D. degree in Electrical Engineering from North China Electric Power University (NCEPU), Baoding, China, in 2005 and 2013, respectively. He is currently a Professor with the Department of Electrical Engineering, NCEPU and the State Key Laboratory of Alternate Electrical Power System with Renewable Energy Sources, Baoding and Beijing, China. He is the Director of Smart Energy Network Integrated Operation Research Center (SENIOR) and the leader of "Double First-Class" research team project at NCEPU. He was a Visiting Professor with the Department of Electrical and Computer Engineering, University of Illinois at Urbana-Champaign, Urbana, IL, USA, from 2016 to 2017. He was a Researcher with the Department of Electrical Engineering, Tsinghua University, Beijing, China, from 2014 to 2016.

Prof. Wang is an Editor of the *IEEE Transactions on Sustainable Energy*, an Editor of the *IEEE Power Engineering Letters*, an Associate Editor of the *IET Renewable Power Generation*, an Editor of the *IEEE Open Access Journal of Power and Energy and Protection and Control of Modern Power Systems*. He was the Guest Editor for the Special Issue on "Demand Side Management and Market Design for Renewable Energy Support and Integration" of *IET Renewable Power Generation*. He is an IEEE Senior Member and the Expert Member of IEC SC8A/WG2. He supervised more than 60 Post-docs, Ph.D. and M.Sc. students. He has authored or coauthored more than 220 publications, including 80 journal papers. His research interests include renewable energy power, electricity price and electricity load forecasting; demand response and electricity market; smart grid; microgrid; and integrated energy system. He was the recipient of the 2020 Science and Technology Progress First Award of Hebei Province, 2018 Technical Invention First Award of Hebei Province, the 2018 Patent Third Award of Hebei Province, the 2014 Natural Sciences Academic Innovation Achievement Award of Hebei Province, the 2018 China Electric Power Science and Technology Progress Third Award, and the 2014 Outstanding Doctoral Dissertation Award of NCEPU. He was the General Chair of the 2017 International Seminar of Renewable Energy Power Forecasting and Absorption Technology and 2018 International Seminar of Integrated Energy and Smart Microgrid Technology.



Gang Qiu received the B.S. degree from Tianjin University, Tianjin, China, in 2000, the M.S. degree from Beijing JiaoTong University, Beijing, China, in 2007. Currently, he is a senior engineer with the Dispatch and Control Center, State Grid Xinjiang Electric Power Co., Ltd, Urumqi 830018, China. He has long been engaged in new energy operation control, power forecasting mid- and long-term power safety verification, and large-scale power grid operation analysis and control.



Yu Li is a professor of engineering with the Dispatch and Control Center, State Grid Xinjiang Electric Power Co., Ltd, Urumqi 830018, China. He is the Standing Director of IEEE PES Energy Storage Technical Committee (China) Energy Storage Market and Planning Subcommittee, the Member of Energy Industry Wind Power Grid-connected Standards Committee. He has long been engaged in large-scale power grid operation analysis and control, energy storage planning, and network source load storage.



Liangzhong Yao received his MSc and PhD degrees in Electrical Engineering from Tsinghua University, China, in 1989 and 1993, respectively. He is now a Professor in the School of Electrical Engineering and Automation at Wuhan University, China. Before joining the Wuhan University in 2019, he had respectively worked at Tsinghua University, University of Manchester (former UMIST), ABB UK Ltd, Alstom Grid UK, and State Grid Corporation of China, from 1993 to 2019. His research fields cover renewable energy grid integration and control, energy storage, and HVDC and DC grid technologies.



Miadreja Shafie-khah (M'13, SM'17) received the M.Sc. and Ph.D. degrees in Electrical Engineering from Tarbiat Modares University, Tehran, Iran, in 2008 and 2012, respectively. He received his first postdoc from the University of Beira Interior (UBI), Covilha, Portugal in 2015. He received his second postdoc from the University of Salerno, Salerno, Italy in 2016.

Currently, he is an Associate Professor at the University of Vaasa, Vaasa, Finland. He was considered one of the Outstanding Reviewers of the IEEE TRANSACTIONS ON SUSTAINABLE ENERGY, in 2014 and 2017, one of the Best Reviewers of the IEEE TRANSACTIONS ON SMART GRID, in 2016 and 2017, and one of the Outstanding Reviewers of the IEEE TRANSACTIONS ON POWER SYSTEMS, in 2017 and 2018. His research interests include power market simulation, market power monitoring, power system optimization, demand response, electric vehicles, price forecasting and smart grids.



João P. S. Catalão (M'04-SM'12) received the M.Sc. degree from the Instituto Superior Técnico (IST), Lisbon, Portugal, in 2003, and the Ph.D. degree and Habilitation for Full Professor ("Agregação") from the University of Beira Interior (UBI), Covilha, Portugal, in 2007 and 2013, respectively. Currently, he is a Professor

at the Faculty of Engineering of the University of Porto (FEUP), Porto, Portugal, and Research Coordinator at INESC TEC. He was also appointed as Visiting Professor by North China Electric Power University, Beijing, China. He was the Primary Coordinator of the EU-funded FP7 project SiNGULAR ("Smart and Sustainable Insular Electricity Grids Under Large-Scale Renewable Integration"), a 5.2-million-euro project involving 11 industry partners. He has authored or coauthored more than 700 publications, including 275 journal papers (more than 80 IEEE Transactions/Journal papers), 372 conference proceedings papers, 5 books, 35 book chapters, and 14 technical reports, with an h-index of 47, an i10-index of 197, and over 8500 citations (according to Google Scholar), having supervised more than 70 post-docs, Ph.D. and M.Sc. students. He is the Editor of the books entitled "Electric Power Systems: Advanced Forecasting Techniques and Optimal Generation Scheduling" and "Smart and Sustainable Power Systems: Operations, Planning and Economics of Insular Electricity Grids" (Boca Raton, FL, USA: CRC Press, 2012 and 2015, respectively). His research interests include power system operations and planning, hydro and thermal scheduling, wind and price forecasting, distributed renewable generation, demand response and smart grids.

Prof. Catalão is an Editor of the IEEE Transactions on Smart Grid, an Editor of the IEEE Transactions on Power Systems, an Associate Editor of the IEEE Transactions on Industrial Informatics. From 2011 till 2018 (seven years) he was an Editor of the IEEE Transactions on Sustainable Energy and an Associate Editor of the IET Renewable Power Generation. He was also a Subject Editor of the IET Renewable Power Generation. He was the Guest Editor-in-Chief for the Special Section on "Real-Time Demand Response" of the IEEE Transactions on Smart Grid, published in December 2012, the Guest Editor-in-Chief for the Special Section on "Reserve and Flexibility for Handling Variability and Uncertainty of Renewable Generation" of the IEEE Transactions on Sustainable Energy, published in April 2016, the Corresponding Guest Editor for the Special Section on "Industrial and Commercial Demand Response" of the IEEE Transactions on Industrial Informatics, published in November 2018, and the Lead Guest Editor for the Special Issue on "Demand Side Management and Market Design for Renewable Energy Support and Integration" of the IET Renewable Power Generation, to be published in March 2019. He was the recipient of the 2011 Scientific Merit Award UBI-FE/Santander Universities, the 2012 Scientific Award UTL/Santander Totta, the 2016 and 2017 FEUP Diplomas of Scientific Recognition, the 2017 Best INESC-ID Researcher Award, and the 2018 Scientific Award ULisboa/Santander Universities, in addition to an Honorable Mention in the 2017 Scientific Award ULisboa/Santander Universities. Moreover, he has won 4 Best Paper Awards at IEEE Conferences.